HHS Public Access

Author manuscript

Cell Rep. Author manuscript; available in PMC 2016 May 08.

Published in final edited form as:

Cell Rep. 2015 August 4; 12(5): 726–733. doi:10.1016/j.celrep.2015.06.062.

Endogenous Glucagon-like peptide-1 suppresses high-fat food intake by reducing synaptic drive onto mesolimbic dopamine neurons

Xue-Feng Wang[1,4], **Jing-Jing Liu**[1,4], **Julia Xia**[1,4], **Ji Liu**[1], **Vincent Mirabella**[1], and **Zhiping P. Pang**[1,2,3,*]

[1]Child Health Institute of New Jersey, Rutgers Robert Wood Johnson Medical School, New Brunswick, NJ 08901

[2]Department of Neuroscience and Cell Biology, Rutgers Robert Wood Johnson Medical School, New Brunswick, NJ 08901

[3]Department of Pediatrics, Rutgers Robert Wood Johnson Medical School, New Brunswick, NJ 08901

SUMMARY

Glucagon-like peptide-1 (GLP-1) and its analogs act as appetite suppressants and have been proven to be clinically efficacious in reducing body weight in obese individuals. Central GLP-1 is expressed in a small population of brainstem cells located in the nucleus tractus solitarius (NTS), which project to a wide range of brain areas. However, it remains unclear how endogenous GLP-1 released in the brain contributes to appetite regulation. By using chemogenetic tools, we discovered that central GLP-1 acts on the midbrain ventral tegmental area (VTA) and suppresses high-fat food intake. We used integrated pathway tracing and synaptic physiology to further demonstrate that activation of GLP-1 receptors specifically reduces the excitatory synaptic strength of dopamine (DA) neurons within the VTA that project to the nucleus accumbens (NAc) medial shell. These data suggest that GLP-1 released from NTS neurons can reduce highly palatable food intake by suppressing mesolimbic DA signaling.

INTRODUCTION

The central glucagon-like peptide-1 (GLP-1) system plays a crucial role in the control of food intake (Turton et al., 1996). GLP-1 signaling is among the most promising targets in the brain for treating overeating disorders (Alhadeff et al., 2012; Dossat et al., 2013; Drucker et al., 2008; Meeran et al., 1999; Secher et al., 2014; Sisley et al., 2014). GLP-1 analogs

[*]**Corresponding author:** Zhiping P. Pang Ph.D., Child Health Institute of New Jersey, Room 3277, 89 French Street, New Brunswick, NJ 08901, Phone: 1-732-235-8074, Zhiping.Pang@rutgers.edu.

[4]These authors contributed equally to this study.

Authors Contribution

X.W. and J.J.L. conducted the electrophysiological, morphological, and behavioral experiments; J.X. conducted behavioral and morphological experiments; J. L. conducted Exendin 9 experiments, Immunohistochemical analysis and performed statistical analysis of the data; V.M. contributed significantly data interpretation and writing of the manuscript. Z.P.P. designed the study and wrote the manuscript. All authors contributed to the writing of the paper.

have been used to treat type 2 diabetes (For review see Lovshin and Drucker, 2009), and a GLP-1 receptor (GLP-1R) agonist, Saxenda (liraglutide), has recently been approved to treat obesity (U.S. Food and Drug Administration, 2014). Central GLP-1 is mainly secreted by a small group of neurons located within the nucleus tractus solitarius (NTS) in the brainstem. GLP-1 expressing neurons project broadly to other brain regions including the hypothalamus, the ventral tegmental area (VTA) and the nucleus accumbens (NAc) (Gu et al., 2013). Accordingly, expression of GLP-1Rs has been detected in many brain areas such as the VTA and NAc (Merchenthaler et al., 1999). Nevertheless, it is still not fully understood how release of central GLP-1 within the brain regulates food intake.

Regulatory mechanisms underlying the control of feeding may be divided into two categories — homeostatic (i.e., hunger-induced feeding to maintain energy balance) and reward-related (i.e., hedonic or pleasure-driven acquisition of highly palatable food). Feeding behavior is ultimately determined by a complex interaction between the two (Liu et al., 2015). Hedonic eating has become a key cause of weight gain and obesity. Therefore, there is a pressing need to further investigate the role of reward circuitry in the regulation of feeding behavior (Volkow et al., 2011). The neural circuits governing food intake intertwine with those mediating reward, and the midbrain dopaminergic (DA) system has been suggested to play a pivotal role in the regulation of reward-related behaviors, including eating (Liu et al., 2015; Volkow et al., 2011). Several studies report that pharmacologic manipulations of GLP-1 signaling, i.e., using GLP-1 analogue Exendin 4 (Exn4) or GLP-1R blocker Exendin 9 (Exn9) infusions, in the VTA (Dickson et al., 2012; Mietlicki-Baase et al., 2013), NAc (Alhadeff et al., 2012; Dossat et al., 2013; Dossat et al., 2011), NTS (Alhadeff and Grill, 2014) and the hippocampus (Hsu et al., 2015), affect the appetitive and motivational aspects of feeding. Together these findings suggest that GLP-1 signaling may affect hedonic food intake. Nevertheless, the neural basis of such effect remains enigmatic.

Utilizing chemogenetic tools, we demonstrated that endogenously released GLP-1 from the NTS is sufficient to suppress high-fat (HF) food intake. More specifically, we found that activation of NTS-originating GLP-1 nerve terminals in the VTA is sufficient to suppress HF food intake. Furthermore, we uncovered that GLP-1R activation directly impedes excitatory synaptic drive onto VTA-to-NAc medial shell projecting DA neurons. Thus, GLP-1 released from NTS neurons may reduce highly palatable food intake through suppression of mesolimbic DA signaling.

RESULTS

Chemogenetic activation of GLP-1 expressing neurons suppresses food intake

To precisely target GLP-1 expressing neurons in the NTS, we took advantage of Phox2b-Cre BAC transgenic mice which express Cre-recombinase in GLP-1 containing neurons within the NTS (Scott et al., 2011). Adeno-associated virus (AAV) expressing Cre-activated yellow fluorescent protein (YFP) was injected into the NTS of Phox2b-Cre animals to specifically visualize GLP-1 neurons (Figures 1A,B and S1). We employed chemogenetics to address whether the activation of NTS GLP-1 neurons affects food intake by expressing designer receptors exclusively activated by designer drugs (DREADDs). Specifically, we expressed Cre-activated hM_3Dq or hM_4Di DREADDS in the NTS of Phox2b-Cre mice through local

stereotactic injections of AAVs. Upon binding to clozapine-N-oxide (CNO), a synthetic agonist of DREADDs, Gq-coupled hM_3Dq activates neuronal burst firing while Gi-coupled hM_4Di inhibits neuronal firing (Sternson and Roth, 2014). By genetically encoding these designer receptors into GLP-1 neurons in the NTS (Figures S1B-D), we were able to control the activity of these neurons in a temporal and spatial manner and evaluate the subsequent impact on feeding behavior.

Immunostaining showed that neurons in the NTS expressing these DREADDs or YFP also express GLP-1 (Figure S1). To assay food intake behavior, animals were given *ad libitum* access to both standard rodent chow and a highly palatable HF diet (Van Heek et al., 1997). Daily food intake was measured for 5 days before performing chemogenetic experiments, in order to establish a stable baseline of food consumption, intraperitoneal (i.p.) CNO injections were then performed for three consecutive days as experimental trials (Figures 1C and D). Activation of NTS GLP-1 neurons by CNO in Gq-coupled hM_3Dq-expressing animals led to significant decreases in HF food intake compared to control mice expressing mCherry alone (Figures 1D and E). Interestingly, the same procedure showed little effect on standard chow intake (Figures S2A-C). This is in contrast to the behavior induced by pharmacological activation of GLP-1 receptors by Exn4 (Alhadeff et al., 2012). The activation of NTS GLP-1 neurons had little impact on body weight within 24 hours after application of CNO (Figures S2D), which is consistent with results from deletion of neuronal GLP-1Rs (Sisley et al., 2014). Conversely, hM_4Di-expressing mice showed increased HF diet intake (Figures 1E, S2 and S3), suggesting that inhibition of NTS GLP-1 neurons can facilitate food intake.

To unequivocally define the specific involvement of GLP-1 signaling in the suppression of HF food intake, we pre-administered GLP-1R antagonist Exn9 before the application of CNO in a subset of hM_3Dq-expressing animals. Remarkably, we found that the food intake suppression induced by CNO activation of hM_3Dq receptors was blocked, indicating that appetite suppression was specifically achieved by activating GLP-1 release from hM_3Dq-expressing NTS neurons (Figure 1F). The terminals of NTS GLP-1 neurons projecting to VTA express vGluT2 (Zheng et al., 2014) but not vGluT1 (Figure S4A), thus they may also release glutamate. However, our data provide strong evidence that endogenous GLP-1 released from NTS neurons projecting to the VTA suppresses food intake.

GLP-1 release in the VTA regulates high fat food intake

We next asked if GLP-1 signaling within the mesolimbic system is involved in regulating HF food intake. Consistent with previous reports (Dickson et al., 2012; Mietlicki-Baase et al., 2013), we demonstrated that intra-VTA infusion of Exn4 produced profound HF food intake suppression relative to control animals undergoing saline injections (Figures 2A and B). Therefore, we speculate that the VTA is a critical component of the neural circuitry through which GLP-1 controls reward-driven food intake. Next, we sought to use DREADDs to induce the release of GLP-1 from the nerve terminals. The hM_3Dq is a Gq-coupled DREADD and its activation stimulates the production of inositol triphosphate and diacylglycerol (Pei et al., 2008), both of which are known to increase synaptic vesicle release at the nerve terminal (Nakamura et al., 1999; Rhee et al., 2002). We injected CNO

directly into the VTA of hM_3Dq-mCherry, hM_4Di-mCherry and mCherry-expressing mice (Figure S4B), and observed whether CNO altered food intake behavior. Interestingly, consistent with results from microinjections of Exn4 into the VTA (Figure 2B), local chemogenetic activation of GLP-1 nerve terminals in the VTA in hM_3Dq-expressing mice significantly suppressed HF food intake (Figures 2C-F). We cannot exclude the possibility that action potentials generated by CNO at the nerve terminals might back propagate to the cell body and then possibly release GLP-1 in other brain regions. However, our data suggest that suppression of food intake by hM_3Dq and CNO is at least partially mediated by locally released GLP-1. Infusion of CNO into the VTA did not produce altered feeding behavior in hM_4Di expressing mice (Figure S4C–D), suggesting that dampening GLP-1 signaling in the VTA alone may not be sufficient to induce the acute overeating response observed after broader suppression of all GLP-1 neurons by i.p. injections of CNO (Figure 1E). Our data therefore demonstrate that local activation of NTS projections in the VTA is likely sufficient to decrease HF food intake, supporting the hypothesis that central GLP-1 release can regulate feeding behavior via signaling pathways within the reward centers of the brain.

GLP-1R activation suppresses excitatory synaptic inputs onto the VTA-to-NAc projecting DA neurons

Given that synaptic transmission and plasticity govern information flow in the brain and control behavioral outcomes, we hypothesized that GLP-1 signaling modulates synaptic transmission in the mesolimbic system. We focused on the modulatory effects of GLP-1 in VTA-to-NAc medial shell projecting neurons, which compose a well-established reward pathway (Lammel et al., 2011; Lammel et al., 2012). To identify these neurons, we injected retrograde fluorescent microbeads into the NAc medial shell (Figure 3A). The majority of VTA-to-NAc projecting neurons were DA as shown by detection of tyrosine hydroxylase (TH) by immunohistochemistry (IHC) (Figure 3A). In order to study morphologic and electrophysiologic properties of these neurons, we performed whole cell patch clamp recordings. We included fluorescent dye, either Alexa594-dextran or Alexa488-biocytin, for filling the recorded cells. Neuronal subtypes were identified by *post hoc* IHC for TH (Figures 3B and C). We found that TH^+ DA VTA neurons have more dendritic branchings, smaller *N*-methyl-D-aspartate (NMDA) receptor mediated excitatory postsynaptic currents (EPSCs) and a higher ratio of α-amino-3-hydroxy-5-methyl-4-isoxazolepropionic acid (AMPA) receptor to NMDA receptor mediated EPSCs (i.e., AMPA/NMDA EPSC ratio) (Figure S5). Nevertheless, we found no clear differences in the sizes of hyperpolarization activated cation channel mediated currents (I_h) (Figure S5A) between TH^+ and TH^- VTA-to-NAc projecting neurons. The sizes of I_h have been used for electrophysiologic identification of the VTA DA neurons (Chieng et al., 2011). However, these data suggest that categorizing VTA neurons as DA or non-DA by measuring I_h current alone may not be adequate, as described previously (Ungless and Grace, 2012).

To test whether GLP-1R activation regulates synaptic plasticity within the VTA, we recorded EPSCs in VTA-to-NAc medial shell projecting neurons in the absence or presence of GLP-1R agonist Exn4 (Figures 3–5). Neuronal subtypes were identified by *post hoc* IHC for TH. In TH^+ VTA-to-NAc projecting neurons, application of Exn4 consistently suppressed AMPA receptor mediated EPSCs (Figures 3D and E). However, no significant change was

found in NMDA EPSCs before and after Exn4 application (Figure 3F). These data suggest that postsynaptic modifications reduce the excitatory synaptic strength, most likely through the specific removal of AMPA receptors from the postsynaptic membrane (otherwise NMDA receptor mediated EPSCs would additionally show a reduction after Exn4 application). We then measured the AMPA/NMDA EPSC ratio which suggested modifications in synaptic strength by the insertion/removal of AMPA receptors during long term synaptic plasticity. We found a consistent reduction in the AMPA/NMDA EPSC ratio after the application of Exn4 (Figure 3G), further suggesting a postsynaptic modification.

In order to further delineate the pre- and post-synaptic mechanisms, we first calculated the coefficient of variation of evoked AMPA receptor mediated EPSCs which showed no significant change with application of Exn4, suggesting no obvious alteration in presynaptic release probability. Moreover, we also recorded miniature EPSCs (mEPSCs) and found that the amplitude in DA neurons significantly decreased following application of Exn4 (Figures 4A-C). Additionally, the paired-pulse ratio of evoked EPSCs showed no obvious change before or after Exn4 application (Figure S5I and J), again suggesting unaltered presynaptic vesicle release probability.

In contrast, in TH^- (non-DA) VTA-to-NAc medial shell projecting neurons the application of Exn4 produced minor changes in AMPA and NMDA receptor mediated evoked EPSCs, a moderate increase in the AMPA/NMDA ratio (in contrast to the decrease in TH^+ neurons), and no change in the coefficient of variance of EPSCs (Figures 3C and I-M). Moreover, we did not observe changes in mEPSCs in non-DA neurons (Figures 4D-F). Together with the data from VTA-to-NAc projecting DA neurons, these data suggest a cell type specific effect of GLP-1R activation on synaptic plasticity in the VTA.

Considering that neurons in the VTA also receive inhibitory synaptic inputs which are mediated by GABA (Johnson and North, 1992), we also studied the regulatory effects of GLP-1R activation on inhibitory synaptic inputs onto VTA-to-NAc medial shell projecting neurons. Activation of GLP-1Rs by Exn4 resulted in an increase in the amplitude of spontaneous inhibitory postsynaptic currents (sIPSCs) in DA VTA neurons (Figures 5 A-D). In contrast, GLP-1R activation had no obvious impact on sIPSCs in non-DA neurons (Figures 5E-H). Furthermore, no significant differences were detected in miniature IPSCs (mIPSCs) in the presence of TTX (Figures 5 I and J). Thus, Exn4 may facilitate inhibitory synaptic transmission mediated by spontaneous action potentials in the VTA-to-NAc projecting DA neurons.

DISCUSSION

This study demonstrates that release of endogenous GLP-1 from NTS neurons projecting to the VTA is sufficient to reduce highly palatable food intake in mice. Moreover, we identified that excitatory synaptic drive onto VTA DA neurons projecting to the medial shell of the NAc is specifically suppressed upon GLP-1R activation, implying a down regulation of VTA-to-NAc DA signaling.

GLP-1 receptors are broadly expressed in the brain including the hypothalamus and reward centers such as the NAc and VTA (Merchenthaler et al., 1999). Food intake can be regulated by homeostatic (hunger-driven) signals and hedonic (reward-related) signals, and the mesolimbic DA system is a common neural integrator involved in hedonic food intake control (Kenny, 2011; Volkow et al., 2011). Exogenous application of GLP-1 analogs in the VTA suppresses food intake (Dickson et al., 2012; Mietlicki-Baase et al., 2013). Consistent with these observations, our data show that exogenous application of GLP-1R agonist Exn-4 in the VTA is sufficient to reduce consumption of HF food. We also demonstrate that endogenously released GLP-1 in the VTA is sufficient to reduce HF food intake (Fig. 1). We thus propose that endogenous GLP-1 signaling within the mesolimbic system may be an effective target to manipulate eating behavior.

The mechanisms underlying GLP-1 mediated food intake suppression are not fully understood. Limited reports on the role of GLP-1 in regulating synaptic function show that GLP-1R activation increases firing in hypothalamic orexin/hypocretin neurons by regulating intrinsic membrane properties (e.g., sodium and calcium channel conductance, and spontaneous neurotransmitter release) (Acuna-Goycolea and van den Pol, 2004). In pancreatic-projecting neurons in the brain stem, GLP-1 has been shown to facilitate sEPSC and sIPSC release (Wan et al., 2007). Our data indicate that GLP-1 analog Exn4 regulates synaptic transmission in a cell-type specific and synapse specific manner. Among the VTA-to-NAc medial shell projecting neurons, DA neurons show a decrease in excitatory synaptic strength and a facilitation of inhibitory synaptic inputs upon administration of Exn4 (Figs. 3 and 5). However, non-DA neurons show increased excitatory synaptic strength (without perturbed inhibitory synaptic strength) upon GLP-1R activation (Figs. 4 and 5).

Unequivocal identification of the specific pathways (e.g., VTA to NAc) and cell types (e.g., DA vs. non-DA neurons) is particularly important for interpreting functional information in the VTA because: 1) previous identification of DA neurons within the VTA based on electrophysiological characteristics remains controversial (Ungless and Grace, 2012) and 2) VTA DA neurons projecting to the NAc or prefrontal cortical brain regions have differential responses towards reward and aversion (Lammel et al., 2011; Lammel et al., 2012). Our data support this complexity, although they somewhat contradict results from a previous report showing facilitation of excitatory synaptic transmission by Exn4 in putative DA neurons identified by the sizes of I_h current in the rat VTA (Mietlicki-Baase et al., 2013). The discrepancy could arise from differences in neuronal subtypes, since, as mentioned previously, electrophysiology may not be a reliable method for identifying DA VTA neurons, and projection pathways which were not defined. Of course, species differences may also exist.

Within the core of the NAc, GLP-1Rs seem to have no regulatory effect on DA nerve terminals because application of Exn4 appears to not alter DA release in striatal brain slices lacking midbrain cell bodies (Mietlicki-Baase et al., 2014). These data simply indicate that GLP-1R signaling in the NAc core does not involve local regulation of DA release and are not at all contradictory to our hypothesis that DA released by VTA-NAc projecting neurons functions to reduce appetite by decreasing pleasure and reward derived from palatable food. Support for this hypothesis was provided by a recent study in humans demonstrating that

DA enhances the neural reward response to food, thereby influencing food intake behavior (Medic et al., 2014). We thus hypothesize that endogenous release of central GLP-1 suppresses mesolimbic DA signaling and reduces appetite by decreasing the pleasure and reward derived from palatable food.

We show evidence that excitatory input to VTA-to-NAc medial shell projecting DA neurons is reduced, implying decreased release of DA into the NAc. In exploring the relationships between food intake, GLP-1 signaling, and synaptic transmission within the reward neural circuitry, we provide an integrated perspective that likely has implications for other motivated behaviors, such as drug abuse and addiction (Egecioglu et al., 2013; Shirazi et al., 2013). Further studies examining other brain regions, circuits and cell-types, as well as the underlying molecular mechanisms, are needed to comprehensively understand the role of GLP-1 in regulating food intake and other reward-driven behaviors.

Experimental Procedures

Animals

All procedures involved using mice were approved by the Rutgers Robert Wood Johnson Medical School Institutional Animal Care and Use Committee (IACUC). The Phox2b-Cre mice (Scott et al., 2011) were obtained from Jackson Laboratories (Stock 016223). Wild type mice C57/Bl6 were purchased from the Jackson Laboratories.

Adeno-Associated-Virus (AAV) infection of Nucleus Tractus Solitarius (NTS) neurons

Under isoflurane inhalation anesthesia (VetEquip) and using a stereotaxic instrument (KOPF M1900), Phox2b-Cre mice were injected bilaterally (0.6-1 μl each side) in the NTS (lambda −3.15 mm; lateral ±0.6 mm; ventral 4.15 mm) with either AAV-hSyn-DIO-hM$_4$Di-mCherry, AAV-hSyn-DIO-hM$_3$Dq-mCherry, AAV-hSyn-DIO-mCherry or AAV-DIO-ChR-YFP (UNC GTC Vector Core). The ChR-YFP is membrane bounded and offers good morphological analyses for both the cell bodies and axons of Cre-expressing neurons. Mice were allowed a survival period of 14 days prior to experimental manipulation. Injections sites were confirmed in all animals.

Immunohistochemistry (IHC)

Mice were anesthetized with euthasol and transcardially perfused with 4% paraformaldehyde (PFA) in PBS, pH 7.4. Either coronal or sagittal brain slices (50 μm) were prepared and standard IHC protocol was followed. The primary antibodies used were TH (Affinity-purified rabbit Anti-Tyrosine Hydroxylase 1:1000; Abcam); vGluT1 (mouse monoclonal 1:1000; Abcam); vGluT2 (NeuroMab); GLP-1 (Affinity-purified Chicken Anti-GLP-1, peptide sequences HAEGTFTSDVSSYC; or Peninsula Laboratories T-4363). AlexaFluor secondary antibodies used to visualize the signal using a confocal microscope. For slice physiology post-hoc immunostaining, brain slices were fixed in 4% PFA for 2 hours, then washed in PBS and processed with IHC.

Behavioral test

Mice (7-8 weeks old) were housed on a 12h light (06:00)/dark (18:00) cycle with *ad libitum* access to water, standard chow (Fat 21.635% mouse diet 20, LabDiet) and high fat (HF) diet (45 kcal% Fat, Research Diet) in all behavioral experiments. Note that when mice were given standard chow and HF diet, the animals would consume mainly HF diet. Prior to experiments, animals were housed in individual cages for 3 days. For i.p. and stereotaxic injections with Exn 4 (Tocris, 2.4μg/kg, i.p. and 0.24 μg/kg for intracranial)/ 0.9% saline or CNO (0.3 μg/kg, 100 μl, i.p. and 0.03 μg/kg, 50 μl each side, for intracranial)/ 0.9% saline were performed at the beginning of the dark cycle (start time 18:00 hours). For assaying the involvement of GLP1-R in food intake suppression by NTS GLP1 neuronal activation using chemogenetics, Exn9 (8.4 μg/kg) were injected i.p.15 min prior to i.p. injection of CNO. Exn 4, Exn 9 and clozapine-N-oxide (CNO, Tocris) were stored in aliquots at −20 °C and dissolved in vehicle (0.9% sodium chloride) before use. Food weight was measured at 18:00, 20:00, 23:00, and 06:00 to calculate food intake volume. Intake was adjusted for spillage.

Retrograde Labeling of Ventral Tegmental Area (VTA) to Nucleus Accumbens (NAc) medial shell projecting Neurons

Mice (6-weeks-old) were anesthetized using isoflurane, placed into a stereotactic frame (KOPF M1900), and red or green RetroBeads (100 nl; LumaFluor Inc.) were injected bilaterally in the medial shell region of the NAc (bregma 2.2 mm; lateral ±0.5 mm; ventral 4.5 mm). To allow adequate time for retrograde transport of the RetroBeads to the somata of VTA neurons, mice were allowed to survive for 14 days prior to slice physiology. Injections sites were confirmed in all animals.

Electrophysiological Recordings from Adult Mouse Midbrain

Electrophysiology was performed as described previously (Pang et al., 2002) with modifications. Briefly, mice were deeply anesthetized with Euthasol. Coronal midbrain slices (300 μm) were prepared and whole cell patch clamp recordings were done at 30 °C. Patch pipettes (3.8-4.4 MΩ) were pulled from borosilicate glass and filled with internal solution containing (in mM): 40 CsCl, 10 HEPES, 0.05 EGTA, 1.8 NaCl, 3.5 KCl, 1.7 $MgCl_2$, 2 Mg-ATP, 0.4 Na_4-GTP, 10 Phosphocreatine, 5 QX-314. Alexa594 (Life Technologies) or 0.2% Neurobiotine-488 (Life Technologies) was added to label recorded neurons (pH 7.2, 280-290 mOsm). Whole cell patch clamp recordings were done using Axon 700B amplifier. Data were filtered at 2 kHz, digitized at 10 kHz and collected using Clampex 10.2 (Molecular Devices). To record EPSCs, picrotoxin (50 μM, Sigma) was added to block IPSCs mediated by $GABA_A$ receptors. TTX (1 μM) was added to block action potential for mEPSCs recording. To record inhibitory currents, NMDAR antagonist D-APV (50) μM and AMPAR antagonist CNQX (20) uM, were added to block excitatory currents. A bipolar stimulating electrode was placed 100–300 μm lateral to the recording electrode, and was used to stimulate afferents at 0.05 Hz. Neurons were voltage-clamped at −70 mV to record AMPAR EPSCs or IPSCs and at +40 mV to record dual component EPSCs containing NMDAR EPSCs. AMPAR/NMDAR ratios were also calculated by dividing the peak of the AMPAR EPSC at −70 mV by the value of the NMDAR EPSC after stimulation start time 50ms at +40 mV.

Data analysis

Repeated measures ANOVA and multiple t-test with Bonferroni were used. Student's t-test or paired t-test was used to determine statistical differences. Two-way ANOVA analysis was used for multiple treatments with multiple groups. Statistical significance was set at $p < 0.05$. All data values are presented as means ± SEM.

Supplementary Material

Refer to Web version on PubMed Central for supplementary material.

Acknowledgments

Research in the Pang Laboratory was supported by the Sinsheimer Scholar Foundation, the NJ Health Foundation, the US-Israel Binational Science Foundation (BSF), and the Robert Wood Johnson Foundation. We also thank members of the Pang Laboratory and Drs. Ami Citri, Stephan Lammel and Weiping Han, and Nicholas Bello for critical suggestions.

References

Acuna-Goycolea C, van den Pol A. Glucagon-like peptide 1 excites hypocretin/orexin neurons by direct and indirect mechanisms: implications for viscera-mediated arousal. The Journal of neuroscience : the official journal of the Society for Neuroscience. 2004; 24:8141–8152. [PubMed: 15371515]

Alhadeff AL, Grill HJ. Hindbrain nucleus tractus solitarius glucagon-like peptide-1 receptor signaling reduces appetitive and motivational aspects of feeding. American journal of physiology. Regulatory, integrative and comparative physiology. 2014; 307:R465–R470.

Alhadeff AL, Rupprecht LE, Hayes MR. GLP-1 Neurons in the Nucleus of the Solitary Tract Project Directly to the Ventral Tegmental Area and Nucleus Accumbens to Control for Food Intake. Endocrinology. 2012; 153:647–658. [PubMed: 22128031]

Chieng B, Azriel Y, Mohammadi S, Christie MJ. Distinct cellular properties of identified dopaminergic and GABAergic neurons in the mouse ventral tegmental area. The Journal of physiology. 2011; 589:3775–3787. [PubMed: 21646409]

Dickson SL, Shirazi RH, Hansson C, Bergquist F, Nissbrandt H, Skibicka KP. The Glucagon-Like Peptide 1 (GLP-1) Analogue, Exendin-4, Decreases the Rewarding Value of Food: A New Role for Mesolimbic GLP-1 Receptors. Journal of Neuroscience. 2012; 32:4812–4820. [PubMed: 22492036]

Dossat AM, Diaz R, Gallo L, Panagos A, Kay K, Williams DL. Nucleus accumbens GLP-1 receptors influence meal size and palatability. American Journal of Physiology-Endocrinology and Metabolism. 2013; 304:E1314–E1320. [PubMed: 23612998]

Dossat AM, Lilly N, Kay K, Williams DL. Glucagon-Like Peptide 1 Receptors in Nucleus Accumbens Affect Food Intake. Journal of Neuroscience. 2011; 31:14453–14457. [PubMed: 21994361]

Drucker DJ, Buse JB, Taylor K, Kendall DM, Trautmann M, Zhuang D, Porter L, Group D-S. Exenatide once weekly versus twice daily for the treatment of type 2 diabetes: a randomised, open-label, non-inferiority study. Lancet. 2008; 372:1240–1250. [PubMed: 18782641]

Egecioglu E, Steensland P, Fredriksson I, Feltmann K, Engel JA, Jerlhag E. The glucagon-like peptide 1 analogue Exendin-4 attenuates alcohol mediated behaviors in rodents. Psychoneuroendocrinology. 2013; 38:1259–1270. [PubMed: 23219472]

Gu GB, Roland B, Tomaselli K, Dolman CS, Lowe C, Heilig JS. Glucagon-like peptide-1 in the rat brain: Distribution of expression and functional implication. Journal of Comparative Neurology. 2013; 521:2235–2261. [PubMed: 23238833]

Hsu TM, Hahn JD, Konanur VR, Lam A, Kanoski SE. Hippocampal GLP-1 receptors influence food intake, meal size, and effort-based responding for food through volume transmission. Neuropsychopharmacology : official publication of the American College of Neuropsychopharmacology. 2015; 40:327–337. [PubMed: 25035078]

Johnson SW, North RA. Two types of neurone in the rat ventral tegmental area and their synaptic inputs. The Journal of physiology. 1992; 450:455–468. [PubMed: 1331427]

Kenny PJ. Reward Mechanisms in Obesity: New Insights and Future Directions. Neuron. 2011; 69:664–679. [PubMed: 21338878]

Lammel S, Ion DI, Roeper J, Malenka RC. Projection-specific modulation of dopamine neuron synapses by aversive and rewarding stimuli. Neuron. 2011; 70:855–862. [PubMed: 21658580]

Lammel S, Lim BK, Ran C, Huang KW, Betley MJ, Tye KM, Deisseroth K, Malenka RC. Input-specific control of reward and aversion in the ventral tegmental area. Nature. 2012; 491:212–217. [PubMed: 23064228]

Liu JJ, Mukherjee D, Haritan D, Ignatowska-Jankowska B, Liu J, Citri A, Pang ZP. High on food: the interaction between the neural circutis for feeding and for reward. Front. Biol. 2015

Lovshin JA, Drucker DJ. Incretin-based therapies for type 2 diabetes mellitus. Nature reviews. Endocrinology. 2009; 5:262–269.

Medic N, Ziauddeen H, Vestergaard MD, Henning E, Schultz W, Farooqi IS, Fletcher PC. Dopamine modulates the neural representation of subjective value of food in hungry subjects. The Journal of neuroscience : the official journal of the Society for Neuroscience. 2014; 34:16856–16864. [PubMed: 25505337]

Meeran K, O'Shea D, Edwards CM, Turton MD, Heath MM, Gunn I, Abusnana S, Rossi M, Small CJ, Goldstone AP, et al. Repeated intracerebroventricular administration of glucagon-like peptide-1-(7-36) amide or exendin-(9-39) alters body weight in the rat. Endocrinology. 1999; 140:244–250. [PubMed: 9886831]

Merchenthaler I, Lane M, Shughrue P. Distribution of pre-pro-glucagon and glucagon-like peptide-1 receptor messenger RNAs in the rat central nervous system. The Journal of comparative neurology. 1999; 403:261–280. [PubMed: 9886047]

Mietlicki-Baase EG, Ortinski PI, Reiner DJ, Sinon CG, McCutcheon JE, Pierce RC, Roitman MF, Hayes MR. Glucagon-like peptide-1 receptor activation in the nucleus accumbens core suppresses feeding by increasing glutamatergic AMPA/kainate signaling. The Journal of neuroscience : the official journal of the Society for Neuroscience. 2014; 34:6985–6992. [PubMed: 24828651]

Mietlicki-Baase EG, Ortinski PI, Rupprecht LE, Olivos DR, Alhadeff AL, Pierce RC, Hayes MR. The food intake-suppressive effects of glucagon-like peptide-1 receptor signaling in the ventral tegmental area are mediated by AMPA/kainate receptors. American Journal of Physiology-Endocrinology and Metabolism. 2013; 305:E1367–E1374. [PubMed: 24105414]

Nakamura T, Barbara JG, Nakamura K, Ross WN. Synergistic release of Ca2+ from IP3-sensitive stores evoked by synaptic activation of mGluRs paired with backpropagating action potentials. Neuron. 1999; 24:727–737. [PubMed: 10595522]

Pang ZP, Deng P, Ruan YW, Xu ZC. Depression of fast excitatory synaptic transmission in large aspiny neurons of the neostriatum after transient forebrain ischemia. The Journal of neuroscience : the official journal of the Society for Neuroscience. 2002; 22:10948–10957. [PubMed: 12486190]

Pei Y, Rogan SC, Yan F, Roth BL. Engineered GPCRs as tools to modulate signal transduction. Physiology. 2008; 23:313–321. [PubMed: 19074739]

Rhee JS, Betz A, Pyott S, Reim K, Varoqueaux F, Augustin I, Hesse D, Sudhof TC, Takahashi M, Rosenmund C, et al. Beta phorbol ester- and diacylglycerol-induced augmentation of transmitter release is mediated by Munc13s and not by PKCs. Cell. 2002; 108:121–133. [PubMed: 11792326]

Scott MM, Williams KW, Rossi J, Lee CE, Elmquist JK. Leptin receptor expression in hindbrain Glp-1 neurons regulates food intake and energy balance in mice. The Journal of clinical investigation. 2011; 121:2413–2421. [PubMed: 21606595]

Secher A, Jelsing J, Baquero AF, Hecksher-Sorensen J, Cowley MA, Dalboge LS, Hansen G, Grove KL, Pyke C, Raun K, et al. The arcuate nucleus mediates GLP-1 receptor agonist liraglutide-dependent weight loss. The Journal of clinical investigation. 2014; 124:4473–4488. [PubMed: 25202980]

Shirazi RH, Dickson SL, Skibicka KP. Gut peptide GLP-1 and its analogue, Exendin-4, decrease alcohol intake and reward. PloS one. 2013; 8:e61965. [PubMed: 23613987]

Sisley S, Gutierrez-Aguilar R, Scott M, D'Alessio DA, Sandoval DA, Seeley RJ. Neuronal GLP1R mediates liraglutide's anorectic but not glucose-lowering effect. The Journal of clinical investigation. 2014; 124:2456–2463. [PubMed: 24762441]

Sternson SM, Roth BL. Chemogenetic tools to interrogate brain functions. Annual review of neuroscience. 2014; 37:387–407.

Turton MD, O'Shea D, Gunn I, Beak SA, Edwards CM, Meeran K, Choi SJ, Taylor GM, Heath MM, Lambert PD, et al. A role for glucagon-like peptide-1 in the central regulation of feeding. Nature. 1996; 379:69–72. [PubMed: 8538742]

U.S. Food and Drug Administration. SAXENDA NDA 206321,REMS approval letter. 2014 Dec. 2014.

Ungless MA, Grace AA. Are you or aren't you? Challenges associated with physiologically identifying dopamine neurons. Trends in neurosciences. 2012; 35:422–430. [PubMed: 22459161]

Van Heek M, Compton DS, France CF, Tedesco RP, Fawzi AB, Graziano MP, Sybertz EJ, Strader CD, Davis HR Jr. Diet-induced obese mice develop peripheral, but not central, resistance to leptin. The Journal of clinical investigation. 1997; 99:385–390. [PubMed: 9022070]

Volkow ND, Wang GJ, Baler RD. Reward, dopamine and the control of food intake: implications for obesity. Trends in Cognitive Sciences. 2011; 15:37–46. [PubMed: 21109477]

Wan S, Coleman FH, Travagli RA. Glucagon-like peptide-1 excites pancreas-projecting preganglionic vagal motoneurons. American journal of physiology. Gastrointestinal and liver physiology. 2007; 292:G1474–G1482. [PubMed: 17322063]

Zheng H, Stornetta RL, Agassandian K, Rinaman L. Glutamatergic phenotype of glucagon-like peptide 1 neurons in the caudal nucleus of the solitary tract in rats. Brain structure & function. 2014

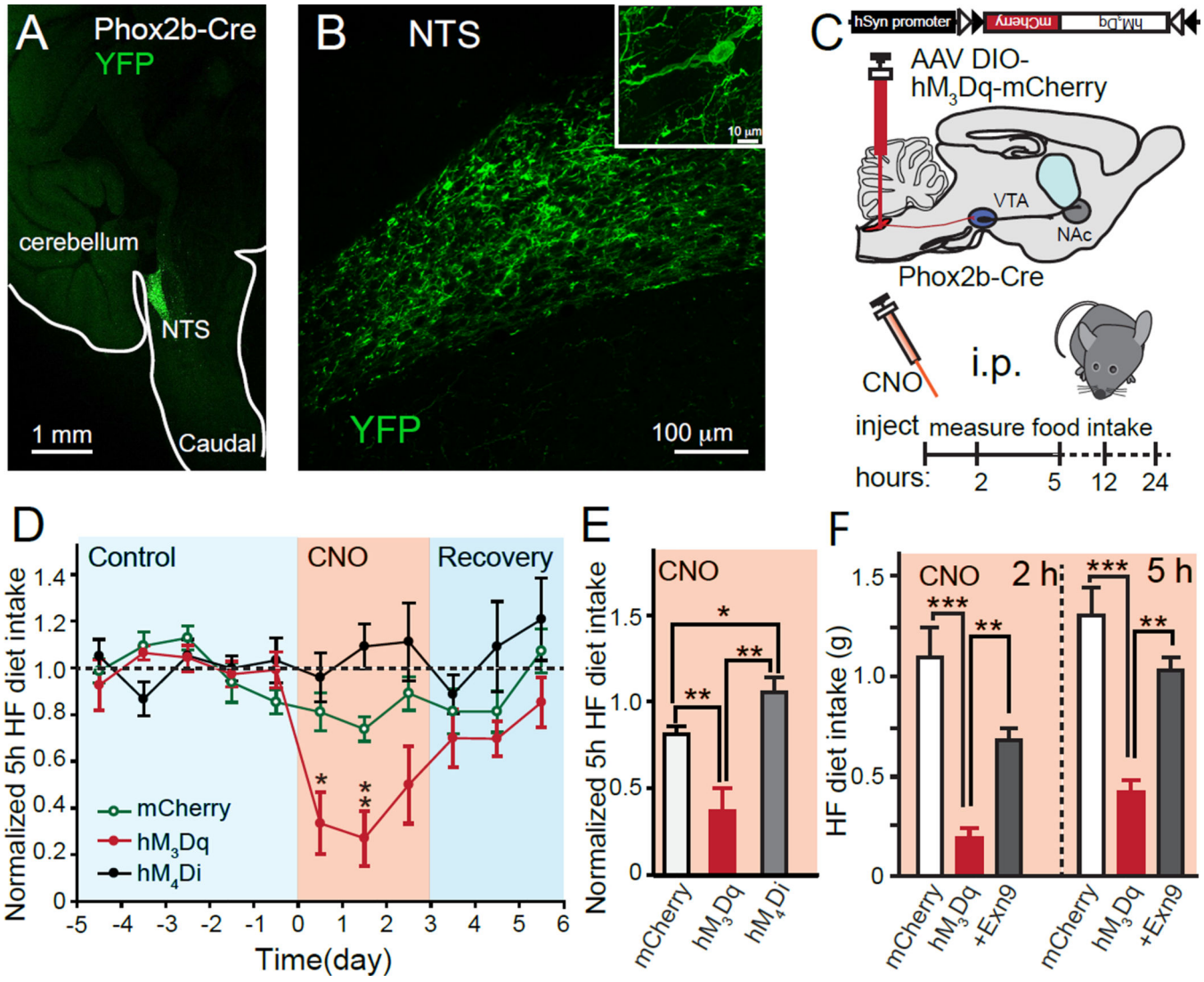

Figure 1. Activation of NTS GLP-1 neurons releases GLP-1 and reduces high-fat (HF) diet intake

(**A,B**) Representative sagittal mouse brain section showing viral infection of NTS neurons with Cre-dependent AAV-DIO-Channelrhodopsin-YFP in Phox2b-Cre mice (**C**) Illustration depicts Phox2b-Cre animals injected with AAV DIO-DREADDs (hM_3Dq) and timeline of experiments (**D-F**). (**D**) Normalized HF diet intake measured 5h after i.p. injection of either PBS (control/recovery) or CNO. There was an overall time effect ($p<0.05$) and time×group effect ($p<0.001$); *post hoc* t-tests were used for individual time points comparison. (**E**) Normalized HF diet intake at 5h during CNO i.p. injection period only (mCherry n=7, hM_3Dq n=7, hM_4Di n=6). Average HF diet intake over three days of CNO application was normalized to the averages of the baseline (5 days). Absolute food intake amount in different groups at different times are shown in Suppl. Fig. 2. Student t-tests were used. (**F**) HF diet intake suppression induced by hM_3Dq activation is blocked by the specific GLP-1 receptor antagonist Exendin-9 (Exn9). (mCherry n=7; hM_3Dq n=6; Exn9 n=6). Exn9 was applied 15 min before the application of CNO. There was an overall time effect ($p<0.001$), group effect

($p<0.001$) and time×group effect ($p<0.001$); ANOVA 2 hr $p<0.001$; *post hoc* Bonferroni: mCherry vs. hM_3Dq $p<0.001$; mCherry vs. hM_3Dq+Exn9 $p=0.051$; hM_3Dq vs. hM_3Dq +Exn9, $p=0.002$. ANOVA 5hr: $P<0.001$; *post hoc* Bonferroni: mCherry vs hM_3Dq: $p<0.001$, mCherry vs. hM_3Dq+Exn9: $p=0.227$, hM_3Dq vs. hM_3Dq+Exn9: $p=0.002$. All values represent mean ± SEM. *$p<0.05$, **$p<0.01$, *** $p<0.001$

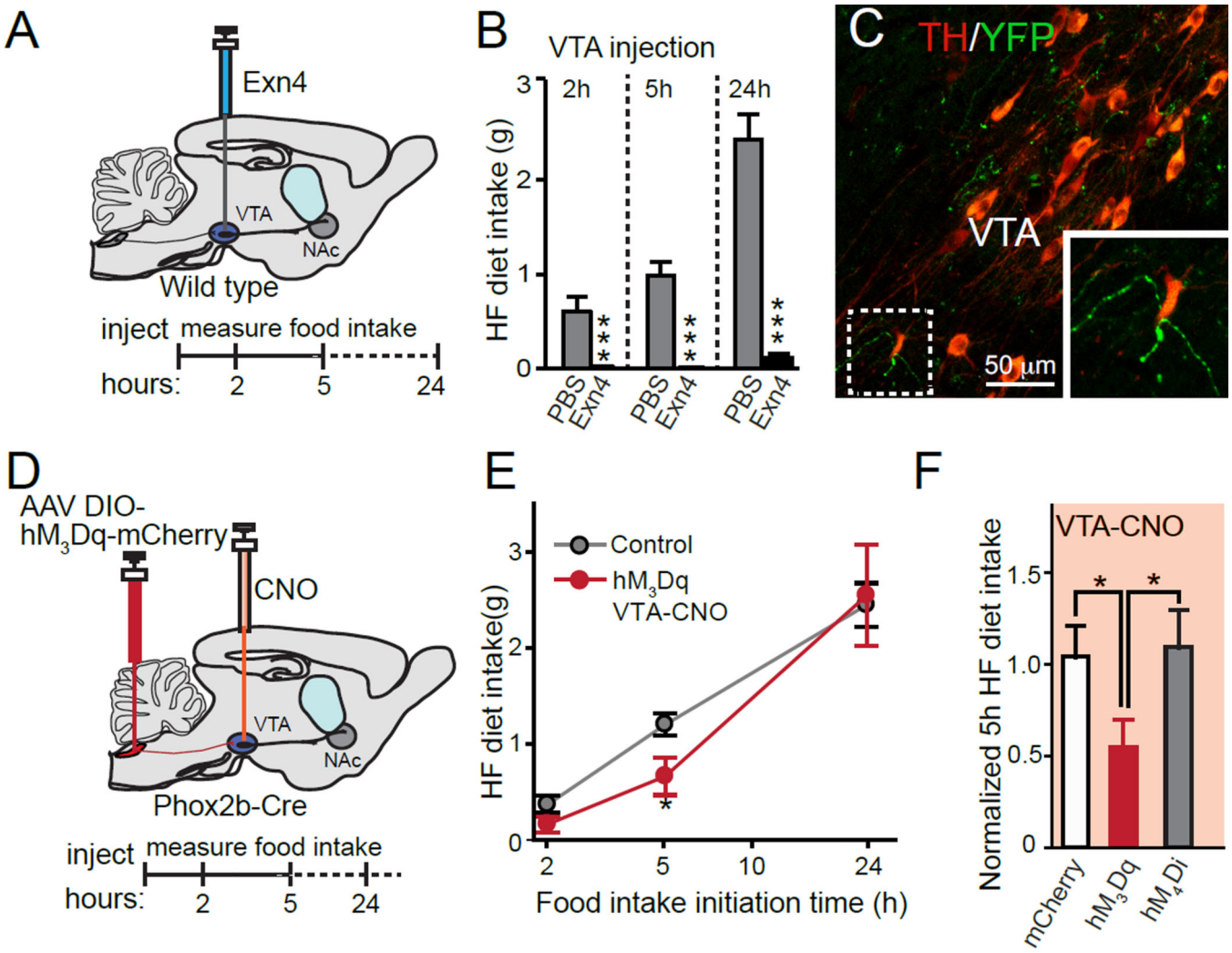

Figure 2. Activation of VTA GLP-1 nerve terminals reduces HF diet intake

(**A**) Illustration showing the injection of Exn4 directly into VTA. (**B**) Food intake at 2h, 5h and 24h after bilateral microinjections of PBS (n=5) or Exendin-4 (Exn4, n=5) into the VTA of wild type mice. Repeat measurement: time: $p<0.001$; group: $p<0.001$; time×group: $p<0.001$. (**C**) NTS axons (green) visible in VTA region immunostained for tyrosine hydroxylase (red). (**D**) Illustration showing the injection of AAV DIO-DREADDs into the NTS region of Phox2b-Cre animals and CNO infusion into VTA brain region of AAV injected animals. (**E**) Plot of HF diet intake from hM3D mice (red) after injection of CNO in VTA compared to control levels of HF diet intake (grey) that were measured 1-day prior to injections. There was an overall time effect ($p<0.001$) and time×group effect ($p<0.001$). (**F**) HF diet intake 5h after injection of CNO into VTA in mice expressing mCherry (white, n=7), hM_3Dq (red, n=7), or hM_4Di (grey, n=7). Student t-tests were used. All values represent mean ± SEM. *$p<0.05$, **$p<0.01$ *Post hoc* t-tests were used.

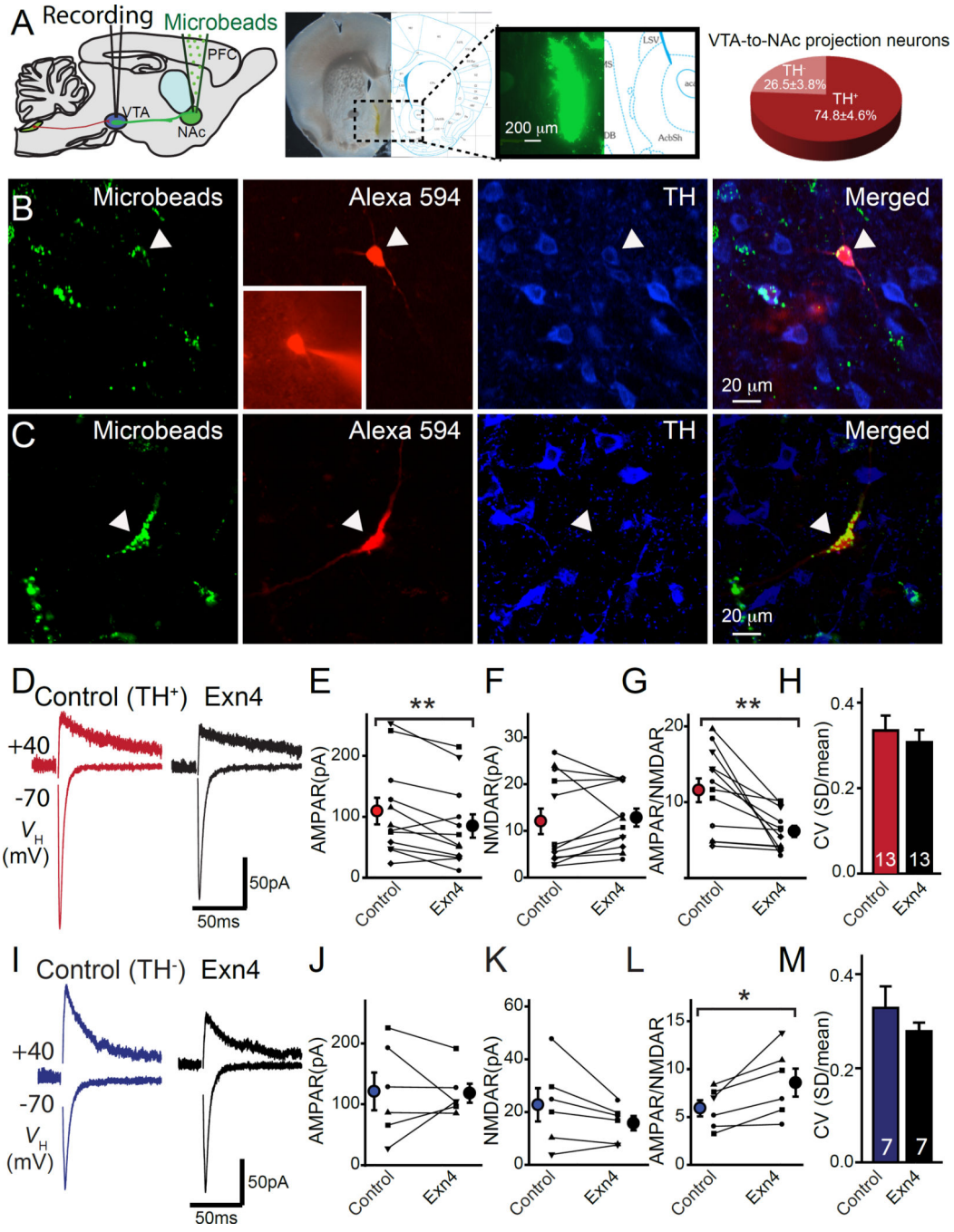

Figure 3. Exendin-4 (Exn4) suppresses excitatory synaptic strength of dopaminergic VTA-NAc neurons

(A) *Left panel*: Schematic illustration of stereotaxic injection of fluorescent microbeads in NAc. Middle: Representative image of NAc injection site. *Right panel*: Statistical distribution of TH^+ and TH^- VTA-to-NAc medial shell projecting neurons. (**B**) Confocal images of recorded retrograde labeled neurons in VTA that were labeled with Alexa 594 *post-hoc* immunostained for tyrosine hydroxylase (TH). **(C)** Representative confocal image of a non-DA (TH^-) VTA-to-NAc projecting neuron. Green=microbeads, red=Alexa 594,

blue=TH. (**D**) Sample AMPAR and NMDAR response at +40mV from DA VTA-to-NAc neurons before (red) and after (black) bath application of Exn4. **(E-H)** Statistical results of AMPAR (**E**), NMDAR (**F**), AMPAR/NMDAR (**G**), and coefficient of variation (**H**)**,** from evoked recordings of TH^+ VTA-to-NAc projecting neurons (n=13). (**I**) Sample AMPAR and NMDAR response at +40mV from non-DA (TH^-) VTA-to-NAc neurons before (blue) and after (black) bath application of Exn4. (**J**-**M**) Statistical results of AMPAR(**J**), NMDAR (**K**), AMPAR/NMDAR (**L**), and coefficient of variation (**M**) (n=7), from evoked response recordings of non DA VTA-to-NAc projection neurons (n=7). All values represent mean ± SEM. Note that paired t-tests were used to define the statistical significances. *p<0.05, **p<0.01.

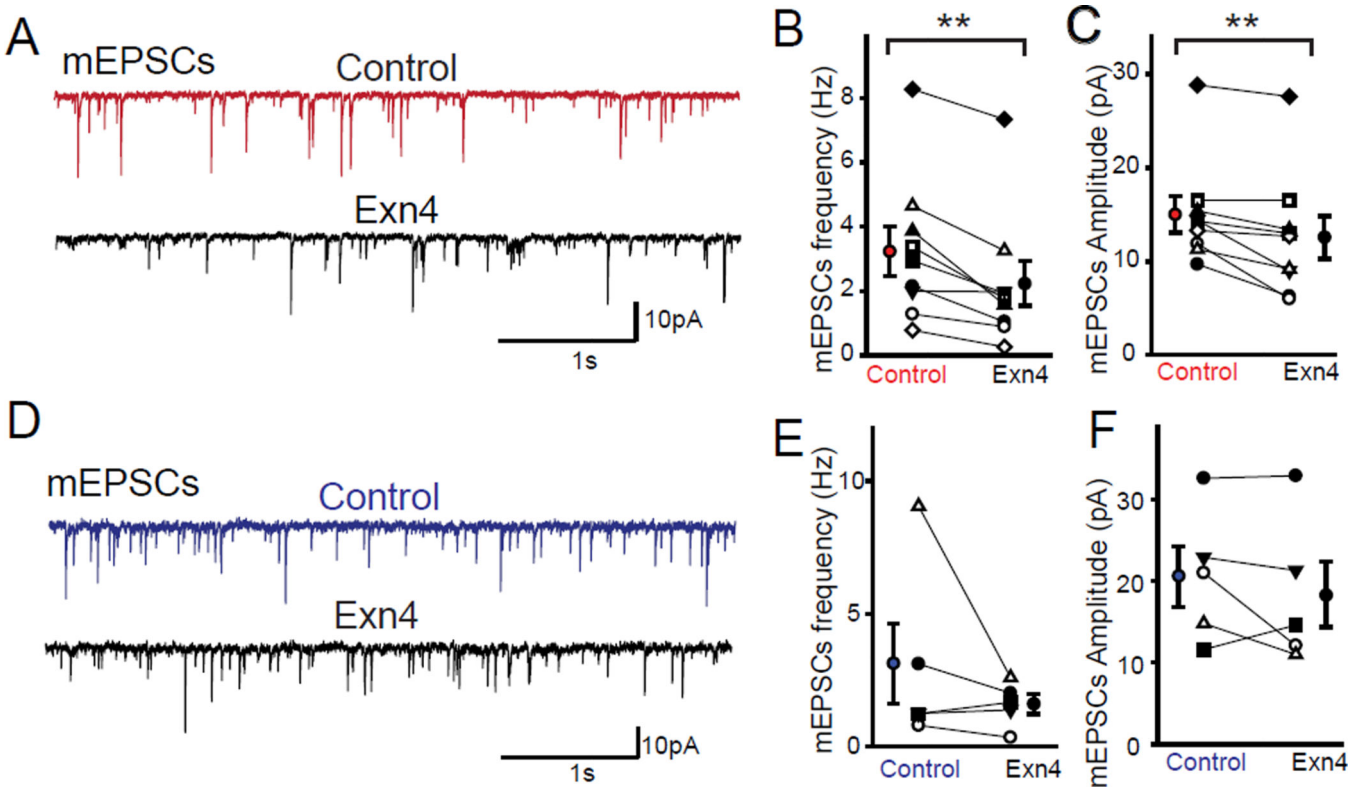

Figure 4. Exendin-4 (Exn4) regulates miniature synaptic releases at excitatory synapses in VTA-to-NAc projection neurons

(**A**) Sample traces of mini EPSCs recorded from DA VTA-NAc neurons before (red) and after (black) bath application of Exn4. (**B**) Frequency and (**C**) amplitude of mEPSCs in VTA-to-NAc projection DA neurons (n=9). (**D**) Sample recordings of mEPSCs in non-DA neurons before and after Exn4 application. (**E**) Frequency and (**F**) amplitude of mEPSCs in non-DA VTA-to-NAc projecting neurons (n=5). All values represent mean ± SEM. Note that paired t-tests were used to define the statistical significances. **p<0.01.

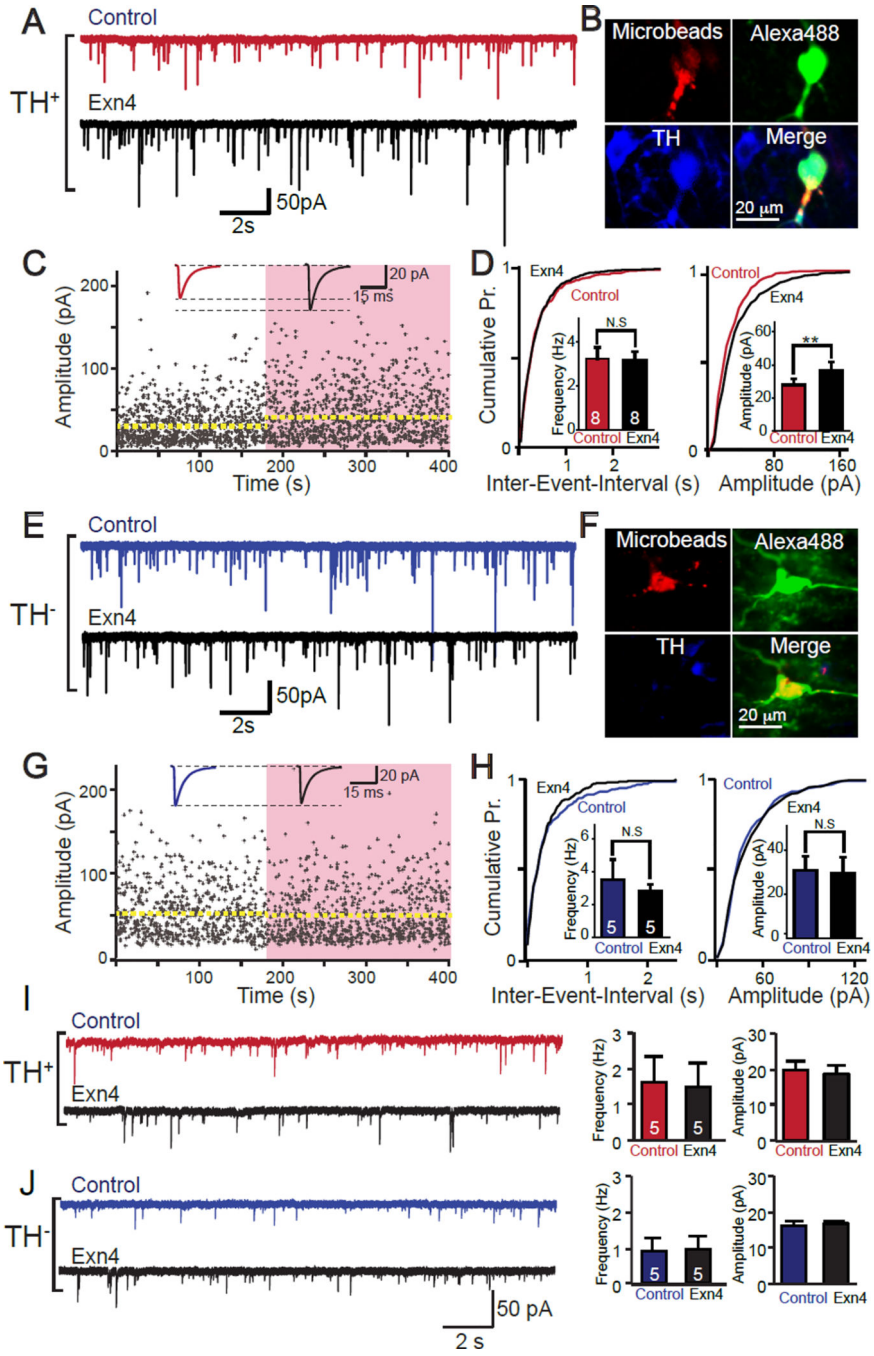

Figure 5. Effects of Exendin-4 (Exn4) on VTA-NAc neuron response to inhibitory inputs

(**A**) Sample recordings of TH$^+$ neurons before and after bath application of Exn4. (**B**) Confocal images of representative TH$^+$ VTA-NAc recorded neuron labeled with microbeads from NAc (*upper left*) or Alexa 488-biocytin from recording electrode (upper right) and immunostained for tyrosine hydroxylase (TH, *lower left*). (**C**) sIPSCs amplitude of TH$^+$ VTA-NAc neurons, before (white) and after (pink shaded area) bath application Exn4, top trace showing the average trace of events before (red) and after (black) application of Exn4. (**D**) Statistical results of sIPSC recordings from (**A**)(n=8). (**E**) Sample recordings of TH$^-$

neurons before and after bath application of Exn4. (**F**) Confocal images of representative TH^- VTA-to-NAc projecting neurons recorded that were labeled with retrobeads from NAc (*upper left*) and Alexa 488-biocytin from recording electrode (*upper right*) and immunostained for tyrosine hydroxylase (TH, *lower left*). (**G**) sIPSCs amplitude of TH^- VTA-NAc neurons before (white) and after (pink shaded area) bath application of Exn4 (top trace showing the average trace of events before and after application of Exn4). (**H**) Statistical results of sIPSC recordings from (**E**) (n=5). (**I** &**J**) Impact of Exn4 on mIPSCs in TH^+ VTA-to-NAc projecting neurons (**I**) and TH^- VTA-to-NAc projection neurons (**J**). *Left panel:* representative traces before and after Exn4; *Right Panel:* pooled data of average frequencies and amplitudes of mIPSCs (n=5 in both groups). Data are presented as mean ± SEM. Note that paired t-tests were used to define the statistical significances. **p<0.01.